Effective control of optical purity by chiral HPLC separation for ester-based liquid crystalline materials forming anticlinic smectic phases

Terézia Vojtylová-Jurkovičová,[a*] Petra Vaňkátová,[a,b] Magdalena Urbańska,[c] Věra Hamplová,[a] David Sýkora [d] and Alexej Bubnov [a]

[a.] Institute of Physics of the Czech Academy of Sciences, Na Slovance 1999/2, 182 21 Prague, Czech Republic.

[b.] Department of Analytical Chemistry, Faculty of Science, Charles University, Albertov 6, 128 43 Prague, Czech Republic.

[c.] Faculty of Advanced Technologies and Chemistry, Military University of Technology, Gen. Sylwestra Kaliskiego 2 Str., 00-908 Warsaw, Poland.

[d.] Department of Analytical Chemistry, Faculty of Chemical Engineering, University of Chemistry and Technology, Technická 5, 166 28 Prague, Czech Republic.

Author for correspondence (*):

Terézia Vojtylová Jurkovičová

Institute of Physics of the Czech Academy of Sciences

Na Slovance 1999/2

182 21 Prague 8

Czech Republic

e-mail: vojtyl@fzu.cz

phone: +420-266052781

Abstract

Currently, effective control of optical purity by chiral separation of (*S*) and (*R*) enantiomers remains a relevant and highlighted task when designing new chiral organic materials in general, especially for self-assembling materials possessing synclinic and anticlinic smectic phases. An efficient methodology for accomplishing this task was developed and verified with a series of chiral fluorinated liquid-crystalline materials with lateral substitution on the molecular core. The self-assembling behaviour of new racemic materials was established. Upon cooling from the isotropic phase, all materials possessed orthogonal, synclinic and anticlinic smectic mesophases. The materials were available with four fluorine substitution patterns and in racemic and pure (*R*) and (*S*) enantiomer forms. Chiral high-performance liquid chromatography was accomplished using polysaccharide-based chiral stationary phases. All separations were performed in normal chromatographic mode, and the baseline separation of all enantiomer pairs was achieved using chiral stationary phases based on derivatized amylose and cellulose. The enantiomer elution order for racemic mixtures was verified by comparing their retention times with those of the respective pure (*R*) and (*S*) enantiomers. Interestingly, two materials demonstrated an unexpected switch in enantiomer elution order. This is very important information that is useful, for instance, for potential utilization in preparative scale chiral chromatography.

Keywords: high-performance liquid chromatography, self-assembling behaviour, fluorinated materials, chiral liquid crystals, chiral separation, racemic mixtures

Introduction

Chirality, based on molecular symmetry elements, is present in many regular systems in nature [1], and it is widely used in artificially designed systems as part of smart functional organic materials utilized in various applications. Enantiomers (or stereoisomers) can exhibit significantly diverse properties in chiral environment. Moreover, there is growing evidence that chirality can also induce unique characteristics of artificially designed materials and devices [2, 3] based on such materials. In reality, starting materials and intermediates available for the synthesis of chiral substances are often not perfectly optically pure. In most cases, a low percentage of the opposite enantiomer (impurity) is present. Moreover, a partial racemization of the intermediates during a specific synthetic step can be another considerable source of the optical purity decrease. In the past, optical purity was determined primarily by optical rotation measurements, which does not allow obtaining sufficiently accurate information on trace amounts of the pollutant stereoisomer. In many cases, the enantiomeric purity of the compounds was not documented in the literature or with insufficient precision and accuracy.

High-performance liquid chromatography (HPLC) using chiral stationary phases (CSPs) is a highly versatile technique broadly applied in the field of chiral separations and analysis of various racemic mixtures of organic materials. Moreover, chiral HPLC is regularly used for estimation of the optical purity of chiral materials [4-7]. The main aim of enantioseparation is to separate enantiomers with sufficient resolution within the shortest possible time, keeping the acquisition and operating costs as low as possible while obtaining reliable and reproducible results.

Direct enantioseparation employing chiral stationary phases has become the most often used approach for separating enantiomers. The CSP contains well-defined chiral centres, making them available for stereoselective interactions with enantiomers of analytes. This may result in different retention of the individual enantiomers on the column and, thus, their separation. Chiral sorbents based on derivatives of the polysaccharides amylose and cellulose are the most widespread and highly successfully utilized CSPs; they provide very broad applicability and excellent separation selectivity [8]. There are numerous situations where it is necessary to assess the enantiomeric excess of the target material with high precision and accuracy. A practical example of the successful utilization of chiral HPLC includes the determination of the enantiomeric ratio of lactic acid for the diagnosis of metabolic acidosis for medical diagnostic purposes [9]. This technique is also widely used in the pharmacology and pharmaceutical industries [10-18], in agrochemistry to control chiral pesticides for agricultural needs [19, 20] or in environmental studies to determine the occurrence and composition of pollutants or their residues in the environment [21-25].

The self-assembling behaviour of liquid crystalline (LC) and fluid materials is highly sensitive to the presence of optically contaminating impurities [26]. The optical purity of such materials affects not only the helical pitch but also the order and stability of the mesophases [1, 27-36].

Currently, investigation of new chiral LC materials with different ratios of (*R*) and (*S*) enantiomers is an exciting and highlighted topic [5, 6, 31-34, 37]. However, it is necessary to carry out two multistage syntheses to obtain both pure enantiomers. Unfortunately, this procedure often does not give high yields of the intermediates and final products, and it can also be very time-consuming. A way to make this procedure more efficient might be to use the racemic material instead (it is usually significantly less expensive than the enantiomers) as the initial material to carry out a synthetic procedure followed by separation of two enantiomeric forms on the preparative scale by applying a chiral column to obtain (*R*) and (*S*) enantiomers in their pure forms. The utilization and confirmation of the applicability of this concept is one of the main objectives of the present investigations.

Chiral LC materials possessing the anticlinic phase with polar order are widely studied for their “smart” mesomorphic and electro-optic properties [38-41]. Such antiferroelectric liquid crystals (AFLCs) can be used as smart materials for high-definition micro-displays and other photonic devices. The main advantages of antiferroelectric materials for specific use in display devices are a fast response, a broad grey scale, and a possibility of a passive matrix scheme and the innovation of large flat-panel displays [27, 42-47]. The properties of the self-assembling materials might be predicted and controlled [48-50]. Unfortunately, AFLC materials suffer from two disadvantages. First, there is a problem with proper alignment of the antiferroelectric phase while obtaining a high-quality dark state. The second problem consists of the existence of a “so-called” pre-transitional effect, which is a weak linear electro-optic effect active under applied fields below the threshold for the switching response [45, 51-53]. However, the first challenge can be solved by designing multicomponent mixtures from components with the same chiral terminal chain but with opposite helical twisting [54, 55]. The second problem can be solved by using orthoconic AFLC materials in which the molecular director tilts by 45° with respect to the smectic layer normal. LCs with lateral fluorine substitution possess low conductivity, low viscosity and high thermal stability and can be synthesized both with and without a chiral moiety [28, 56-60], which makes the effective tuning of the mesomorphic and electro-optic behaviour possible by mixing [37, 38, 61-67].

The enantioseparation of racemic AFLC mixtures by liquid chromatography with chiral stationary phases is required if the optical purity should be evaluated and guaranteed. There is no doubt that the mesomorphic properties of AFLC materials are significantly affected by their optical purity when the chiral centre is present in the molecular structure of the LCs [68-70]. Employing HPLC with various CSPs is a very efficient separation method suitable for enantioseparation of various types of chiral compounds [71-73]. Common AFLC materials are relatively large elongated molecules possessing a bulky achiral section and a much smaller chiral moiety; therefore, the enantiomeric recognition of material often remains quite challenging. To the best of our knowledge, there are only a few works devoted to (i) determining the optical purity of AFLC materials by chiral HPLC [74-77] and (ii) preparing highly optically pure AFLC materials [38, 64, 78, 79].

It is essential to know the elution order of the enantiomers, which can be determined by comparing the retention times of the racemic material with those of the pure individual enantiomers. Knowledge of the enantiomer elution order (EEO) is required for the determination of the amount of optical impurities and elucidation of the separation mechanism, and it is also indispensable for preparative chromatography purposes. Generally, at least three types of EEO reversal phenomena in chiral chromatography have been previously described: the first type is a sample-load reversal, the second type is a temperature-induced reversal and the last is a solvent-induced reversal [80, 81]. Recent studies on EEO reversal consider various chemical compounds that are usable as drugs or agrochemicals [82-85].

Recently, [86], we focused on the development of a chiral separation method suitable for a series of LC materials possessing both long and short alkyl spacers in the terminal chain of the molecule and with different positions of laterally substituted fluorine atom(s) in the molecule. Chiral selector chemistry, mobile phase composition, and temperature have been optimized. In the present study, we applied a similar chiral separation protocol, but the method had to be modified to make it suitable for chiral separation of newly synthesized smectic materials with anticlinic ordering. Chiral chromatography experiments revealed that materials with two laterally substituted fluorine atoms exhibited an unexpected switch of the EEO. This was essential information important for the determination of the optical purity of AFLC materials. The exact mechanism of this effect is not yet fully understood.

Materials and methods

Materials under investigation

The general chemical structure of the designed racemic materials and the specification of the lateral substituent (X_1X_2) type and position are presented in Table 1. A series of structurally similar LC materials was designed and synthesized, specifically in the racemic form, denoted as 6.X_1X_2(*RAC*). Pure (*R*) and (*S*) enantiomers, denoted as 6.X_1X_2(*R*) or 6.X_1X_2(*S*) were designed recently [56, 87]. For all materials, the number of carbons in the alkyl spacer of the non-chiral terminal chain of the molecule was equal to six (Table 1).

The efficient synthetic procedure leading to (*R*,*S*) 4'-(1-methylheptyloxycarbonyl)biphenol, an intermediate product for racemic mixtures, was described in detail in ref. [58]. Commercially available (*R*,*S*)-2-octanol with a purity of 99.5% was used. The synthetic protocol for the preparation of the final racemic mixtures is described in refs. [28, 88] and is similar to the synthetic route for pure enantiomers [56, 57, 87, 89-91].

The purity of the precursors was checked by an HP-6890N gas chromatograph with an MS HP5973N detector (both Agilent Technologies, USA) using a Zebron ZB-5 (Phenomenex, USA) chromatographic column with a 30 m length, 0.25 mm i.d., and 0.25 μm film thickness. The purity of LC esters was evaluated using a Prominence HPLC chromatograph coupled with a 2010EV mass spectrometric detector equipped with an electrospray ionization source (both Shimadzu, Japan). The chromatographic conditions used were as follows: the mobile phase consisted of methanol with water 90/10 (v/v), and the flow rate was 0.2 $mL \cdot min^{-1}$. The separation was carried out with a Luna C18 column (150 × 4.6 mm i.d., 3 μm, Phenomenex, USA) at 40 °C.

Mesomorphic behaviour

The mesomorphic properties, i.e., the sequence of mesophases of the newly synthesized esters were studied by observation of characteristic textures and their changes in an Eclipse E600POL (Nikon, Japan) polarizing optical microscope (POM) on planar 12-μm-thick cells in bookshelf geometry. The cells (two glass slides with ITO transparent 5 × 5 mm electrodes on the inner side) for texture observations were supplied by the Military University of Technology (Warsaw, Poland). The cells were filled with the studied materials in the isotropic phase by means of capillary action. An LTS E350 (Linkam, UK) heating/cooling stage equipped with a TMS 93 temperature programmer was used for the temperature control, enabling temperature stabilization within ± 0.1 °C.

The phase transition temperatures were determined precisely by differential scanning calorimetry (DSC) using a DSC 8000 calorimeter (PerkinElmer, USA). Samples of approximately 3-7 mg, hermetically sealed in aluminium pans, were placed into the calorimeter chamber filled with nitrogen. Temperature and enthalpy change values were calibrated on the extrapolated onset temperatures and the enthalpy changes of the melting points of water, indium and zinc. Calorimetric measurements were performed on cooling/heating runs at a rate of 5 $°C \cdot min^{-1}$.

Chiral separation experiments

Two columns with chiral selectors based on derived amylose were used for chiral separations, specifically a Lux 3u Amylose-2 (LA) column (150 × 4.6 mm i.d., 3 μm. Phenomenex, USA) with amylose *tris*(5-chloro-2-methylphenylcarbamate) and a Chiralpak AD-3 (CP) column (150 × 4.6 mm i.d., 3 μm, Daicel, Japan) with amylose *tris*(3,5-dimethylphenylcarbamate) as the chiral selector. Both columns were equipped with appropriate guard columns. One column with a chiral selector based on derived cellulose was employed, a Chiralcel OJ (OJ) column (250 × 4.6 mm i.d., 10 μm, Daicel, Japan) with cellulose *tris*(4-methylbenzoate) as the chiral selector and without a guard column. Mobile phases (MPs) were filtered using a filtration set from Sigma Aldrich (Sigma Aldrich, Czech Republic) and MS PTFE membrane filters (Membrane Solutions, Japan) with a pore size of 0.45 μm. All chiral separations were accomplished with an HPLC system equipped with an Alpha high-pressure pump (ECOM, Czech Republic), a CT050 column temperature controller (AZ Chrom, Slovak Republic), and an ECDA2000 diode array detector (Watrex, Czech Republic). All samples were prepared at 0.1 $mg \cdot mL^{-1}$ concentrations in MP, and the injection volume was 20 μL. The flow rate of the MP was set at 1.0 $mL \cdot min^{-1,}$ and the columns were maintained at 20 °C for the amylose-based chiral stationary phase and 40 °C for the cellulose-based chiral phase. Chromatograms were acquired at a wavelength of 272 nm, which is the absorption maximum of the analysed materials dissolved in the MP. Clarity Chromatography Station (DataApex, Czech Republic) was used for data acquisition and evaluation. Mixtures of n-hexane (Hex) with isopropyl alcohol (IPA) in a 98/2 (v/v) ratio with or without added trifluoroacetic acid (TFA) were used as the mobile phase.

Results and discussion

Mesomorphic properties of LC materials

For newly designed chiral liquid crystalline racemic esters, the sequences of phases were determined by observation of characteristic textures and their changes in POM. The phase transition temperatures and transition enthalpies were evaluated with high accuracy from DSC heating and cooling runs. Specifically, the sequence of phases and phase transition temperatures, the measured cooling, melting point m.p., and clearing point, c.p., measured heating and the respective phase transition enthalpies, ΔH, obtained by DSC for all studied compounds are summarized in Table 2. The mesomorphic behaviour of the related (*R*) and (*S*) enantiomers is also shown, and the comparison of the mesomorphic behaviour of the racemic materials and enantiomers reveals a very good correspondence of the existing mesophases. The minor difference in the phase transition temperatures can be explained by a slight difference between the purity of the racemic materials and the purity of the corresponding enantiomers.

The DSC plots on heating/cooling runs for selected compounds, namely, for 6.HH(*RAC*), 6.HF(*RAC*), 6.FH(*RAC*), and 6.FF(*RAC*) racemic materials are presented in Figure 1.

All four newly designed racemic ester materials possess orthogonal SmA, synclinic SmC and anticlinic SmC_A phases. Similarly, for pure enantiomers, the temperature range of the SmA phase was found to be very narrow, ranging over a few degrees. The synclinic SmC and the anticlinic SmC_A phases exist over a broad temperature range (up to 100 °C and below room temperature). The highest clearing point was found for non-substituted racemic material in comparison to that of other compounds studied in this work. Nevertheless, the lateral substitution by fluorine atoms definitely suppresses the phase transition temperatures (Table 2). The lowest melting and clearing points were detected for 6.FH(*RAC*) and 6.HF(*R*) materials. With the exception of the lowest temperature region, the sequence of mesophases was the same when comparing (*RAC*) racemates and the (*R*) and (*S*) enantiomers. In the case of 6.HF(*RAC*) and 6.FH(*RAC*), only the phase transition from the synclinic phase to the anticlinic phase was detected by the POM because the intensity of the corresponding DSC peaks was extremely low, approaching the DSC device resolution. This is a common occurrence [38, 40], as the phase transition between two tilted phases is characterized by a very minor structural change. For all racemic materials, the highly ordered smectic phase of crystal modification (which was presented for some of the enantiomers) was absent.

Several examples of the characteristic textures obtained with POM for the 6.HH(*RAC*) ester material is presented in Figure 2. The width of all microphotographs is approximately 250 µm. On cooling, the alignment was considerably better (larger smectic fans) and homogeneous than that obtained on the heating cycle. The birefringence changed considerably with decreasing temperature. The orthogonal SmA phase exhibited typical fan-shaped texture, while the tilted mesophases possessed the broken fan-shaped texture, which appears due to smectic layer shrinkage at the phase transition from the orthogonal to tilted phases [92, 93].

Chiral separation of (R) and (S) enantiomers of LC materials

Chromatographic conditions similar to those of an earlier developed method [86] were applied for the enantioseparation of the new liquid crystalline esters on three different chiral columns. In the case of the LA column, the chromatographic method was not as successful as in the case of the CP and OJ columns. The studied materials contain fluorine in their structure at two different positions: (i) on the aromatic ring in the molecule core and (ii) at the terminal chain of the bulky achiral part of the molecule. We speculate that the reason for the inferior results from the LA column relates to the repulsion between two electronegative elements, the fluorine within the structure of the analyte and the chlorine that is part of the column chiral selector, which led to weaker stereoselective interactions between the stationary phase and the studied compounds. The LC materials interacted more with *tris*(3,5-dimethyl-phenylcarbamate)-modified amylose used in the CP column and *tris*(4-methylbenzoate)-cellulose used in the OJ column than with the *tris*(5-chloro-2-methylphenyl-carbamate) selector utilized in the LA column.

The resolution (R_s) for two enantiomers of a racemic mixture reflects the quality of the chiral separation. The R_s parameter can be defined by equation:

$$R_s = 1.18\left(t_{R2} - t_{R1}\right) / \left(W_{b1} + W_{b2}\right)$$

where t_{R1} and t_{R2} are the retention times of the respective enantiomers and W_{b1} and W_{b2} are the corresponding peak widths at a half peak height, measured in the same units as t_{R1} and t_{R2}. Values of R_s equal to or higher than 1.5 are considered baseline separation, which is generally accepted as the minimal resolution required for accurate and precise determination of the ratio of the separated enantiomers.

Separation with the LA column in a MP consisting of 98/2 (v/v) Hex:IPA for all 6.X_1X_2(*RAC*) materials were not satisfactory; R_s varied in the range of 0.08–0.2. Thus, the enantiomers were only partially separated. The elution order of the enantiomers was verified in all cases by using pure individual (*R*) and (*S*) enantiomers. It was found that the (*S*) enantiomer was eluted first in all cases where EEO could be assessed. The addition of TFA as an MP modifier did not improve the chiral separation.

The results obtained with the CP column were much better that those of the LA column (Figure 3). Baseline separation (R_s>1.5) was successfully achieved for the 6.FF(*RAC*) and 6.FH(*RAC*) racemic materials. For 6.HH(*RAC*), baseline separation was almost obtained (R_s=1.25). The racemic material 6.HF(*RAC*) was only partially separated under the given conditions. An unexpected change in EEO in the chromatograms for 6.HH(*RAC*) and 6.HF(*RAC*) materials was detected, where the first eluted peak belonged to the (*R*) enantiomer. This effect was not observed in the case of 6.FH(*RAC*) and 6.FF(*RAC*) materials.

The addition of TFA as a MP modifier did not have any considerable effect on the chiral separation. The potential influence of the separation temperature on EEO reversal at 10 °C and 35 °C was evaluated for the 6.HH(*RAC*) and 6.HF(*RAC*) racemic materials. Chiral separations at 10 °C exhibited the same EEO as at the optimal separation conditions (20 °C). Enantiomeric resolution values obtained for the two materials at 35 °C were close to zero, and the EEO could not be determined.

OJ was employed as the third column to separate 6.HH(*RAC*) and 6.HF(*RAC*), which were not baseline separated with the CP column. The OJ column indeed provided baseline separation for both 6.HH(*RAC*) and 6.HF(*RAC*) using the MP 98/2 (v/v) Hex:IPA. However, at least partially due to the longer column, the analysis time was approximately 65 minutes for 6.HH(*RAC*) and 80 minutes for 6.HF(*RAC*). The separations were then performed at elevated temperatures (40 °C), and very good results in a reasonable amount of time were obtained. Complete enantioseparation with R_s>2.0 was achieved for both samples while shortening the analysis time to under 35 and 50 minutes for 6.HH(*RAC*) and 6.HF(*RAC*), respectively (Figure 4). The other fluorinated materials were also separated on an OJ column under optimized conditions, but the obtained results were worse than those obtained with the CP column. The EEO was *S*, *R* for all the materials on the OJ column. The addition of TFA to the mobile phase had no substantial effect on the enantioseparation.

Moreover, regarding the effect of analyte structure, interesting trends were observed. Adding fluorine to the phenyl ring of the LC materials led to shortening of the retention times (6.HF(*RAC*), 6.FH(*RAC*) and 6.FF(*RAC*) vs. 6.HH(*RAC*)) on the amylose-based CP column. However, on the cellulose-based OJ column, the longest retention times were observed for 6.HF(*RAC*) and 6.FF(*RAC*), indicating that fluorination at the X_2 position increased the in-column retention. Fluorination at the X_1 position had a detrimental effect on the enantioselectivity when utilizing the OJ column, as shown by comparing the chromatograms for 6.HH(*RAC*) vs. 6.FH(*RAC*) and 6.HF(*RAC*) vs. 6.FF(*RAC*).

Conclusions

Several new self-assembling materials were successfully designed, and they can potentially be used as functional dopants while tuning the properties of multicomponent mixtures [38, 54, 61-63] with definite properties, such as those that are orthoconic [38, 58, 87]. These types of self-assembling materials are very promising for different opto-electronic and photonic applications. A series of semi-fluorinated racemic materials differing in the position of the fluorine atom on the aromatic molecule core was synthesized, and the mesomorphic properties of all materials were studied by POM and DSC. All the designed materials possessed the orthogonal SmA, the synclinic SmC, and the anticlinic SmC_A phases over a reasonably broad temperature range. The mesomorphic properties of the designed racemic materials were in good agreement with those of the pure (*S*) and (*R*) enantiomers [56, 57, 87].

The feasibility of enantioseparation of the newly synthesized materials using chiral HPLC was studied with two amylose-based and one cellulose-based chiral stationary phase. Two of the studied racemic materials, 6.FH(*RAC*) and 6.FF(*RAC*), were successfully baseline separated using a *tris*(3,5-dimethyl-phenylcarbamate) amylose CSP, while the 6.HH(*RAC*) and 6.HF(*RAC*) materials were baseline separated with a *tris*(4-methylbenzoate) cellulose chiral selector. All baseline enantioseparations were achieved by employing a simple mobile phase consisting of hexane with isopropanol, 98/2 (v/v), with no additives. Concerning the elution order of the (*R*) and (*S*) enantiomers, a surprising effect was found for the *tris*(3,5-dimethyl-phenylcarbamate) amylose CSP, where the elution order was dependent on the presence and position of the lateral fluorine substituent in the molecular core. This phenomenon was discovered and described for the first time for this type of material. However, a precise explanation of the observed effect will require further studies.

Effective chromatographic methods for optical purity control were developed and successfully tested on synthesized LC materials. The obtained results and gained information will contribute to a better understanding of the process of chiral separation in general that can be of high interest for a broader organic chemistry and soft matter communities.

Acknowledgements

The authors greatly acknowledge the financial support of the Military University of Technology [grant number PBS 23-895], the Czech Science Foundation [project CSF 19-03564S], EU COST Action [project number CA17139], MEYS [project number 8J20PL008] and by Operational

Programme Research, Development and Education financed by European Structural and Investment Funds and the Czech Ministry of Education, Youth and Sports [project No. SOLID21 - CZ.02.1.01/0.0/0.0/16_019/0000760].

Declaration of interest statement

There are no conflicts to declare.

References

[1] Sako T, Kimura Y, Hayakawa R, et al. Influence of optical purity on the smectic-C*b phase of antiferroelectric liquid crystals. Jpn. J. Appl. Phys. 1996;35:L114-L116.~~ DOI: 10.2174/138527210793351436~~

[2] Amabilino D B, Veciana J. Supramolecular Chiral Functional Materials. In: M. Crego-Calama, D. N. Reinhoudt (Eds.). Supramolecular Chirality, Topics in Current Chemistry, vol 265, Berlin: Springer; 2006. p. 253-302.~~ https://doi.org/10.1007/128_034~~

[3] Tschierske C. Mirror symmetry breaking in liquids and liquid crystals. Liq. Cryst. 2018;45:13-15,2221-2252.

[4] Okamoto Z, Ikai T. Chiral HPLC for efficient resolution of enantiomers. Chem Soc Rev 2008;37:2593-2608.~~ DOI: 10.1039/B808881K~~

[5] Vaňkátová P, Kubíčková A, Cigl M, et al. Ultra-performance chromatographic methods for enantioseparation of liquid crystals based on lactic acid.~~ The~~ J~~ournal of~~ Supercrit~~ical~~ Fluid~~s~~ 2019;146:217-225.~~ https://doi.org/10.1016/j.supflu.2019.02.002~~

[6] Vojtylová T, Kašpar M, Hamplová V, et al. Chiral HPLC for a study of the optical purity of new liquid crystalline materials derived from lactic acid. Phase Transit.~~ions~~ 2014;87:758-769.~~ https://doi.org/10.1080/01411594.2014.893344~~

[7] Poryvai A, Vojtylová-Jurkovičová T, Šmahel M, et al. Determination of optical purity of lactic acid-based chiral liquid crystals and corresponding building blocks by chiral high-performance liquid chromatography and supercritical fluid chromatography. Molecules 2019;24:1099(1-11).~~ DOI:10.3390/molecules24061099~~

[8] Chankvetadze B. Recent trends in preparation, investigation and application of polysaccharide-based chiral stationary phases for separation of enantiomers in high-performance liquid chromatography. Trac - Trend Anal Chem 2020;122:115709(1-13).~~ https://doi.org/10.1016/j.trac.2019.115709~~

[9] Henry H, Marmy C N, Steenhout P, et al. Sensitive determination of D-lactic acid and L-lactic acid in urine by HPLC-tandem mass spectrometry. Biomedic. Chromatogr. 2012;26:425-428.~~ https://doi.org/10.1002/bmc.1681~~

[10] Chandrul K K, Srivastava B. Enantiomeric separation in pharmaceutical analysis: a chromatographic approach. J. Chem. Pharmaceut. Res. 2010;2:923-934.

[11] Zhang Y, Yao S, Zeng H, et al. Chiral separation of pharmaceuticals by high performance liquid chromatography. Curr. Pharm Anal 2010;6:114-130.

[12] Webster G K, Kott L. Method development for pharmaceutical chiral chromatography. In: S. Ahuja, S. Scypinski (Eds.). Separation Science and Technology, Handbook of modern Pharmaceutical Analysis, Elsevier; 2011. p. 251-282. ~~https://doi.org/10.1016/B978-0-12-375680-0.00007-3~~

[13] Christodoulou E A. An Overview of HPLC Methods for the Enantiomer Separation of Active Pharmaceutical Ingredients in Bulk and Drug Formulations. Curr. Org. Chem. 2010;14:2337-2347. ~~DOI: 10.2174/138527210793351436~~

[14] Ferretti R, Zanitti L, Cirilli R. Development of a high-performance liquid chromatography method for the simultaneous determination of chiral impurities and assay of (*S*)-clopidogrel using a cellulose-based chiral stationary phase in methanol/water mode. J. Sep. Sci. 2018;41:1173–1506. ~~https://doi.org/10.1002/jssc.201701191~~

[15] Kadkhodaei K, Forcher L, Schmid M G. Separation of enantiomers of new psychoactive substances by high-performance liquid chromatography. J. Sep. Sci. 2018;41:1173–1506. ~~DOI: 10.1002/jssc.201701239~~

[16] Pisani L, Rullo M, Catto M, et al. Structure–property relationship study of the HPLC enantioselective retention of neuroprotective 7-[(1-alkylpiperidin-3-yl)methoxy]coumarin derivatives on an amylose-based chiral stationary phase. J. Sep. Sci. 2018;41:1173–1506. ~~https://doi.org/10.1002/jssc.201701442~~

[17] Protti M, Vignali A, Sanchez Blanco T, et al. Enantioseparation and determination of asenapine in biological fluid micromatrices by HPLC with diode array detection. J. Sep. Sci 2018;41:1173–1506. ~~https://doi.org/10.1002/jssc.201701315~~

[18] Ianni F, Scorzoni S, Gentili P L, et al. Chiral separation of helical chromenes with chloromethyl phenylcarbamate polysaccharide-based stationary phases. J. Sep. Sci. 2018;41:1173–1506. ~~https://doi.org/10.1002/jssc.201701293~~

[19] Xie J, Zhao L, Liu K, et al. Enantioseparation of four amide herbicide stereoisomers using high-performance liquid chromatography. J. Chrom. A 2016;1471:145–154. ~~https://doi.org/10.1016/j.chroma.2016.10.029~~

[20] Zhang L, Miao Y, Lin Ch. Enantiomeric separation of six chiral pesticides that contain chiral sulfur/phosphorus atoms by supercritical fluid chromatography. J. Sep. Sci. 2018;41:1173–1506. ~~https://doi.org/10.1002/jssc.201701039~~

[21] Huhnerfuss H, Shah M R. Enantioselective chromatography—A powerful tool for the discrimination of biotic and abiotic transformation processes of chiral environmental pollutants. J. Chrom A. 2009;1216:481-502. ~~https://doi.org/10.1016/j.chroma.2008.09.043~~

[22] Li Z, Wu T, Li Q, et al. Characterization of racemization of chiral pesticides in organic solvents and water. J. Chrom. A 2010;1217:5718–5723. ~~doi:10.1016/j.chroma.2010.07.016~~

[23] Pérez-Fernández V, García M A, Marina M L. Chiral separation of agricultural fungicides. J. Chrom. A 2011;1218:6561– 6582. ~~https://doi.org/10.1016/j.chroma.2011.07.084~~

[24] Zhao P, Lei S, Xing M, et al. Simultaneous enantioselective determination of six pesticides in aqueous environmental samples by chiral liquid chromatography with tandem mass spectrometry. J. Sep. Sci. 2018;41:1173–1506. ~~https://doi.org/10.1002/jssc.201701259~~

[25] Zhao P, Wang Z, Li K, et al. Multi-residue enantiomeric analysis of 18 chiral pesticides in water, soil and river sediment using magnetic solid-phase extraction basedon amino modified multiwalled carbon nanotubes and chiral liquidchromatography coupled with tandem mass spectrometry. J. Chrom. A 2018;1568:8–21. ~~https://doi.org/10.1016/j.chroma.2018.07.022~~

[26] Emeršič T, Zhang R, Kos Ž, et al. Sculpting stable structures in pure liquids. Sci.~~ence~~ Adv.~~ances~~ 2019;5:eaav4283(1-8).~~, DOI: 10.1126/sciadv.aav4283~~

[27] Fukuda A, Takanishi Y, Isozaki T, et al. Antiferroelectric chiral smectic liquid crystal. J. Mater. Chem. 1994;4:997–1016. ~~DOI: 10.1039/JM9940400997~~

[28] Żurowska M, Dąbrowski R, Dziaduszek J, et al. Comparison of Racemic and Enantiomeric 4′-(1-Methylheptyloxycarbonyl)Biphenyl4-yl 4-[3-(2,2,3,3,4,4,4-Heptafluorobutoxy)Prop-1-Oxy]Benzoates. Mol. Cryst. Liq. Cryst. 2010;525:239-245. ~~https://doi.org/10.1080/15421401003799995~~

[29] Vaupotič N, Čepič M. Effect of optical purity on phase sequence in antiferroelectric liquid crystals. Phys. Rew. E 2005;71:041701(1-7). ~~https://doi.org/10.1103/PhysRevE.71.041701~~

[30] Kishikawa K, Sugiyama T, Watanabe T, et al. Simple and efficient chiral dopants to induce blue phases and their optical purity effects on the physical properties of blue phases. J. Phys. Chem. B 2014;118:10319−10332.~~ https://doi.org/10.1021/jp506358h~~

[31] Gorecka E, Pociecha D, Čepič M, et al. Enantiomeric excess dependence of the phase diagram of antiferroelectric liquid crystals. Phys. Rev. E 2002;65:061703-14. ~~https://doi.org/10.1103/PhysRevE.65.061703~~

[32] Sasaki Y, Aihara K, Isobe M, et al. Effect of Enantiomeric Excess on the Smectic-C*α – Smectic-C* Phase Transition. Mol. Cryst. Liq. Cryst. 2011;546:209-214. ~~https://doi.org/10.1080/15421406.2011.571163~~

[33] Perkowski P, Ogrodnik K, Żurowska M, et al. Antiferroelectric SmC_A* and ferroelectric SmC* phases in racemic mixture. Phase Transit. 2013;86:138-146. ~~https://doi.org/10.1080/01411594.2012.715304~~

[34] Węgłowska D, Perkowski P, Chrunik M, et al. The effect of dopant chirality on the properties of self-assembling materials with a ferroelectric order. Phys. Chem. Chem. Phys. 2018;20:9211–9220.~~ https://doi.org/10.1039/C8CP01004H.~~

[35] Chu J, Wu L, Guo Y, et al. A series of fluorinated liquid crystals with an alanine residue. Liq. Cryst. 2020;47:465-470.

[36] Walker R, Pociecha D, Storey JMD, et al. The Chiral Twist-Bend Nematic Phase (N^*_{TB}). Chem. Eur. J. 2019;25:13329-13335.

[37] Bubnov A, Podoliak N, Hamplová V, et al. Eutectic behaviour of binary mixtures composed by two isomeric lactic acid derivatives. Ferroelectrics 2016;495:105-115.~~ https://doi.org/10.1080/00150193.2016.1136776~~

[38] Piecek W, Bubnov A, Perkowski P, et al. An effect of structurally non compatible additive on the properties of a long pitch antiferroelectric orthoconic mixture. Phase Transit.~~ions~~ 2010;83:551-563. ~~https://doi.org/10.1080/01411594.2010.499496~~

[39] Hamplová V, Bubnov A, Kašpar M, et al. New ferroelectric and antiferroelectric liquid crystalline materials containing different number of lactate units. Liq. Cryst. 2003;30:627-632. ~~https://doi.org/10.1080/0267829031000010695~~

[40] Hamplová V, Bubnov A, Kašpar M, et al. New antiferroelectric liquid crystalline materials containing a keto group and two lactate groups. Liq. Cryst. 2003;30:1463-1470. ~~https://doi.org/10.1080/02678290310001622506~~

[41] Czerwiński M, Urbańska M, Bennis N, et al. Influence of the type of phase sequence and polymer-stabilization on the physicochemical and electro-optical properties of novel high-tilt antiferroelectric liquid crystalline materials. J Mol. Liq. 20019;288:111057. ~~https://doi.org/10.1016/j.molliq.2019.111057~~

[42] Fukuda A, Fukuda A, Johno M, et al. A novel property caused by frustration between ferroelectricity and antiferroelectricity and its application to liquid crystal displays-frustoelectricity and V-shaped switching. J. Mater. Chem. 1999;9:2051–2080. ~~DOI: 10.1039/A903273H~~

[43] Pandey M B, Verma R, Dhar R. Dielectric and electrooptical properties of antiferroelectric liquid crystalline materials. Israel J. Chem. 2012;52:895–907. ~~https://doi.org/10.1002/ijch.201200041~~

[44] Nishiyama S, Ouchi Y, Takezoe H, et al. Giant electroclinic effect in chiral smectic A phase of ferroelectric liquid crystal. Jpn. J. Appl. Phys. 1987;26:L1787–L1789. ~~https://doi.org/10.1143/JJAP.26.L1787~~

[45] Clark N A, Lagerwall S T. Submicrosecond bistable electro-optic switching in liquid crystals. Appl. Phys. Lett. 1980;36:899–901. ~~https://doi.org/10.1063/1.91359~~

[46] Srivastava A K, Agrawal V K, Dabrowski R, et al. Electro-optical and dielectric relaxation studies of an antiferroelectric liquid-crystal mixture (W-132A). J. Appl. Phys. 2005;98:013543(1-8). ~~https://doi.org/10.1063/1.1968426~~

[47] Milewska K, Drzewiński W, Czerwiński M, et al. Highly tilted liquid crystalline materials possessing a direct phase transition from antiferroelectric to isotropic phase. Mat.~~erials~~ Chem.~~istry and~~ Phys~~ics~~. 2016;171:33–38. ~~https://doi.org/10.1016/j.matchemphys.2016.01.011~~

[48] Karny M, Andrysek J, Bodini A, et al. How to exploit external model of data for parameter estimation? Int. J. Adapt. Control Signal Process. 2006; 20:41-50.

[49] Kárný M, Guy T V, Kracík J, et al. Fully probabilistic knowledge expression and incorporation. Stat.~~istics and its~~ Interface 2014;7:503-515. ~~DOI: 10.4310/SII.2014.v7.n4.a7~~

[50] Kárný M, Guy T V. On support of imperfect Bayesian participants. Intell.~~igent~~ Syst.~~ems~~ Ref.~~erence~~ Libr.~~ary~~ 2012;28:29-56. ~~DOI: 10.1007/978-3-642-24647-0~~

[51] D'Have K, Rudquist P, Lagerwall S T, et al. Solution of the dark state problem in antiferroelectric liquid crystal displays. Appl. Phys. Lett. 2000;76:3528–3530. ~~https://doi.org/10.1063/1.126696~~

[52] Rudquist P, Lagerwall J P F, Meier J G, et al. Tilt plane orientation in antiferroelectric liquid crystal cells and the origin of the pretransitional effect. Phys. Rev. E. 2002;66:061708(1-10). ~~DOI: 10.1103/PhysRevE.66.061708~~

[53] Beccherelli R, Elston S J. Evaluation of optical anisotropy in the pretransitional regime in antiferroelectric liquid crystals. Liq. Cryst. 1998;25:573–577. ~~https://doi.org/10.1080/026782998205859~~

[54] Tykarska M, Czerwiński M, Żurowska M. The temperature and concentration dependence of helical pitch in the mixtures of antiferroelectric compounds with the opposite helical twist sense. Liq. Cryst. 2011;38:561–566.~~ DOI: 10.1080/02678292.2011.558217~~

[55] Kumari S, Das I M L, Dhar R, et al. Thermodynamic and dielectric spectroscopy of a racemic antiferroelectric liquid crystal. J. Mol. Liq. 2012;168:54–60.~~ DOI: 10.1016/j.molliq.2012.01.010~~

[56] Żurowska M, Dąbrowski R, Dziaduszek J, et al. Synthesis and Mesomorphic Properties of Chiral Esters Comprising Partially Fluorinated Alkoxyalkoxy Terminal Chains and a 1-methylheptyl Chiral Moiety. Mol. Cryst. Liq. Cryst. 2008;495:497-509. ~~https://doi.org/10.1080/15421400802432428~~

[57] Żurowska M, Dąbrowski R, Dziaduszek J, et al. Influence of alkoxy chain length and fluorosubstitution on mesogenic and spectral properties of high tilted antiferroelectric esters. J. Mater. Chem. 2011;21:2144–2153. ~~DOI: 10.1039/C0JM02015J~~

[58] Drzewiński W, Dąbrowski R, Czupryński K. Orthoconic Antiferroelectrics. Synthesis and Mesomorphic Properties of Optically Active (S)-(+)-4-(1-Methylheptyloxycarbonyl)phenyl 4'-(Fluoroalkanoyloxyalkoxy)biphenyl-4-carboxylates and 4'-(Alkanoyloxyalkoxy)biphenyl-4- carboxylates. Polish J. Chem. 2002;76:273-284.

[59] Żurowska M, Czerwiński M. The new high tilt mixtures with antiferroelectric phase at a broad temperature range and a long helical pitch. Liq. Cryst. 2017;44:1044–1049.~~ https://doi.org/10.1080/02678292.2016.1256443~~

[60] Morawiak P, Żurowska M, Piecek W. A long-pitch orthoconic antiferroelectric mixture modified by isomeric and racemic homostructural dopants. Liq. Cryst. 2018;45:1451–1459. ~~https://doi.org/10.1080/02678292.2018.1446555~~

[61] Fitas J, Marzec M, Szymkowiak M, et al. Mesomorphic, electro-optic and structural properties of binary liquid crystalline mixtures with ferroelectric and antiferroelectric liquid crystalline behaviour. Phase Transit.~~ions~~ 2018;91:1017-1026. ~~https://doi.org/10.1080/01411594.2018.1506883~~

[62] Fitas J, Marzec M, Kurp K, et al. Electro-optic and dielectric properties of new binary ferroelectric and antiferroelectric liquid crystalline mixtures. Liq. Cryst. 2017;44:1468-1476. ~~https://doi.org/10.1080/02678292.2017.1285059~~

[63] Kurp K, Czerwiński M, Tykarska M, et al. Design of advanced multicomponent ferroelectric liquid crystalline mixtures with sub-micrometer helical pitch. Liq. Cryst. 2017;44:748-756. ~~https://doi.org/10.1080/02678292.2016.1239774~~

[64] Bubnov A, Tykarska M, Hamplová V, et al. Tuning the phase diagrams: the miscibility studies of multilactate liquid crystalline compounds, Phase Transit.~~ions~~ 2016;89:885-893. ~~https://doi.org/10.1080/01411594.2015.1087523~~

[65] Bubnov A, Novotná V, Hamplová V, et al. Effect of multilactate chiral part of the liquid crystalline molecule on mesomorphic behaviour. J~~ournal of~~ Mol~~ecular~~ Struct~~ure~~ 2008;892:151-157. ~~https://doi.org/10.1016/j.molstruc.2008.05.016~~

[66] Kurp K, Czerwiński M, Tykarska M. Ferroelectric compounds with chiral (*S*)-1-methylheptyloxycarbonyl terminal chain – their miscibility and a helical pitch. Liq. Cryst. 2015;42:248-254. ~~https://doi.org/10.1080/02678292.2014.982222~~

[67] Kurp K, Czerwiński M, Tykarska M, et al. Design of functional multicomponent liquid crystalline mixtures with nano-scale pitch fulfilling deformed helix ferroelectric mode demands. J. Mol. Liq. 2019;290:111329. ~~https://doi.org/10.1016/j.molliq.2019.111329~~

[68] Bahr C, Heppke G, Sabaschus B. Chiral-racemic phase-diagram of a ferroelectric liquid-crystal with high spontaneous polarization. Ferroelectrics 1988;84:103–118. ~~https://doi.org/10.1080/00150198808016216~~

[69] Amabilino D B. Chirality at the Nanoscale: Nanoparticles, Surfaces, Materials and More, Weinheim: Wiley-VCH; 2009.

[70] Sasaki Y, Le K V, Aya A, et al. High-resolution calorimetric study of phase transitions in chiral smectic C liquid crystalline phases. Phys. Rev. E 2012;86:061704(1-5). ~~https://doi.org/10.1103/PhysRevE.86.061704~~

[71] Allenmark S, Schurig V. Chromatography on chiral stationary phases. J. Mater. Chem. 1997;7:1955–1963. ~~DOI: 10.1039/A702403G~~

[72] Cancelliere G, D'Acquarica I, Gasparrini F, et al. Twenty years of research on silica-based chiral stationary phases. J. Sep. Sci. 2006;29:770–781. ~~https://doi.org/10.1002/jssc.200500517~~

[73] Lammerhofer M. Chiral recognition by enantioselective liquid chromatography: mechanisms and modern chiral stationary phases. J. Chrom A 2010;1217:814–856. ~~https://doi.org/10.1016/j.chroma.2009.10.022~~

[74] Ossowska – Chruściel M D. A convenient synthesis and the mesomorphic properties of new chiral ferroelectric thiobenzoates. Liq. Cryst. 2004;31:1159–1165. ~~https://doi.org/10.1080/02678290410001724764~~

[75] Ossowska-Chruściel M D. Synthesis and mesomorphic properties of some new chiral thiobenzoates containing three rings. Liq Cryst. 2007;34:195–211. ~~http://dx.doi.org/10.1080/02678290601116217~~

[76] Vojtylová T, Niezgoda I, Galewski Z, et al. A new approach to the chiral separation of novel diazenes. J. Sep. Sci. 2015;38:4211–4215. ~~https://doi.org/10.1002/jssc.201601386~~

[77] Vojtylová T, Hamplová V, Galewski Z, et al. Chiral separation of novel diazenes on a polysaccharide-based stationary phase in the reversed-phase mode. J. Sep. Sci. 2017;38:4211–4215. ~~https://doi.org/10.1002/jssc.201601386~~

[78] Finden J G, Yuh E, Huntley Ch, et al. Ferroelectric liquid crystals induced by dopands with axially chiral 2,2′-spirobiindan-1,1′-dione cores: diether vs. diester side-chains. Liq. Cryst. 2007;34:1095–1106.~~ http://dx.doi.org/10.1080/02678290701528899~~

[79] Cui Q, Lemieux R P. Ferroelectric liquid crystals with axially chiral 2,2′-spirobiindan-1,1′-dione cores. Liq. Cryst. 2013;40:1609–1618.~~ http://dx.doi.org/10.1080/02678292.2012.747705~~

[80] Persson B A, Andersson S. Unusual effects of separation conditions on chiral separations. J. Chrom. A. 2001;906:195-203.~~ doi:10.1016/j.chroma.2011.10.014~~

[81] Chankvetadze B. Recent developments on polysaccharide-based chiral stationary phases for liquid-phase separation of enantiomers. J. Chrom. A 2012;1269:26-51.~~ https://doi.org/10.1016/j.chroma.2012.10.033~~

[82] Gegenava M, Chankvetadze L, Farkas T, et al. Enantioseparation of selected chiral sulfoxides in high-performance liquid chromatography with polysaccharide-based chiral selectors in polar organic mobile phases with emphasis on enantiomer elution order. J. Sep. Sci. 2014;37:1083 – 1088.~~ DOI 10.1002/jssc.201301318~~

[83] Kolderová N, Neveselý T, Šturala J, et al. Enantioseparation of Chiral Sulfoxides on Amylose-Based Columns: Comparison of Normal Phase Liquid Chromatography and Supercritical Fluid Chromatography. Chromatographia 2017;80:547-557. ~~DOI 10.1007/s10337-016-3234-6~~

[84] Yang X, Su L, Hou X, et al. High-performance liquid chromatographic enantioseparation of 3,5-disubstituted hydantoins analogs and temperature-induced reversals of elution orders on a polysaccharide-based chiral stationary phase. J. Chrom. A 2014;1355:291-295.~~ http://dx.doi.org/10.1016/j.chroma.2014.06.022~~

[85] Xiang C, Liu G, Kang S, et al. Unusual chromatographic enantioseparation behavior of naproxen on an immobilized polysaccharide-based chiral stationary phase. J. Chrom. A 2011;1218:8718-8721.~~ https://doi.org/10.1016/j.chroma.2011.10.014~~

[86] Vojtylová T, Żurowska M, Milewska K, et al. Chiral HPLC and physical characterisation of orthoconic antiferroelectric liquid crystals. Liq. Cryst. 2016;43:1244-1250.~~ DOI: 10.1080/02678292.2016.1166401 ~~

[87] Żurowska M, Dziaduszek J, Szala M, et al. Effect of lateral fluorine substitution far from the chiral center on mesomorphic behaviour of highly titled antiferroelectric (*S*) and (*R*) enantiomers. J. of Mol. Liq. 2018;267:504-510. ~~DOI: 10.1016/j.molliq.2017.12.114 ~~

[88] Urbańska M, Dziaduszek J, Strzeżysz O, et al. Synclinic and anticlinic properties of (*R*,*S*) 4’-(1-methylheptyloxycarbonyl)biphenyl-4-yl 4-[7-(2,2,3,3,4,4,4-heptafluorobutoxy)heptyl-1-oxy]benzoates. Phase Transit~~ions~~. 2019;92:657–666. ~~https://doi.org/10.1080/01411594.2019.1616196~~

[89] Urbańska M, Strzeżysz O, Szala M. Highly titled antiferroelectric (*R*) enantiomers useful for the formulation of eutectic mixtures. Liq. Cryst. 2019;47:179-190.~~ https://doi.org/10.1080/02678292.2019.1633585~~

[90] Żurowska M, Czerwiński M, Dziaduszek J, et al. Examination of new chiral smectics with four aromatic rings. Phase Transit~~ions~~. 2018;91:521–529. ~~https://doi.org/10.1080/01411594.2018.1428974~~

[91] Żurowska M, Filipowicz M, Czerwiński M, et al. Synthesis and properties of ferro- and antiferroelectric esters with a chiral centre based on (*S*)-(+)-3-octanol. Liq. Cryst. 2019;46:299–308.~~ https://doi.org/10.1080/02678292.2018.1499147~~

[92] Novotná V, Hamplová V, Bubnov A, et al. First photoresponsive liquid crystalline materials with small layer shrinkage at the transition to the ferroelectric phase. J~~ournal of~~ Mat~~erials~~ Chem~~istry~~ 2009;19:3992-3997.~~ DOI: 10.1039/B821738F~~

[93] Garić M, Bubnov A, Kašpar M, et al. New ferroelectric liquid crystalline materials containing one and two lactate groups attached to the molecule core. Liq. Cryst. 2005;32:565-572.~~ https://doi.org/10.1080/02678290500075134~~

Table(s) with caption(s)

Table 1. General chemical structure of the designed LC materials and their purity. Lateral substitution with a fluorine atom was executed at the X_1 and X_2 positions as indicated. Abbreviations (*RAC*), (*R*), (*S*) represent the racemic material, (*R*)-enantiomer and (*S*)-enantiomer, respectively.

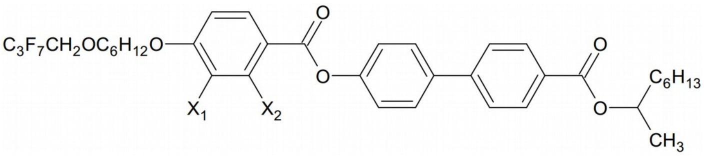

Acronym	**X_1**	**X_2**	Optical purity	**Refs**
6.HH(*RAC*)	H	H	-	-
6.HH(*R*);	H	H	> 99 %;	[87];
-**6.HH(*S*)**			99.99 %	[56, 57, 87]
6.HF(*RAC*)	H	F	-	-
6.HF(*R*);	H	F	> 99 %;	[87];
-**6.HF(*S*)**			98.95 %	[56, 57, 87]
6.FH(*RAC*)	F	H	-	-
6.FH(*R*);	F	H	> 99 %;	[87];
-**6.FH(*S*)**			99.35 %	[56, 57, 87]
6.FF(*RAC*)	F	F	-	-
6.FF(*R*);	F	F	> 99 %;	[87];
-**6.FF(*S*)**			98.5 %	[56, 57, 87]

Table 2. Sequence of phases and phase transition temperatures, T (°C), measured during cooling (5 °C·min^{-1}); clearing point, c.p. (°C) and melting points m.p. (°C), measured during heating (5 °C·min^{-1}) and the corresponding phase transition enthalpies, *ΔH* [kJ·mol^{-1}], obtained by DSC for the studied ester racemates. All the data on related (*R*) and (*S*) enantiomers [56, 57, 87] are given for comparison.

Acronym	**m.p.**	**c.p.**	**phase**	**T [ΔH]**	**phase**	**T [ΔH]**	**phase**	**T [ΔH]**	**phase**	**T [ΔH]**	**phase**	**T [ΔH]**	**Iso**	**Refs**
6.HH(*RAC*)	59.8 [+31.3]	128.6 [+4.4]	**Cr**	1.6 [-8.4]	▬		**SmC$_A$**	103.9 [-0.3]	**SmC**	124.4 [-1.2]	**SmA**	127.5 [-4.3]	**Iso**	-
6.HH(*R*)	62.5 [+23.0]	127.1 [+3.7]	**Cr**	10.5 [-11.4]	▬		**SmC$_A$***	88.6 [-0.01]	**SmC***	124.5 [-1.3]	**SmA***	125.8 [-3.6]	**Iso**	[56, 57, 87]
6.HH(*S*)	62.2 [+22.7]	127.4 [+3.9]	**Cr**	10.3 [-11.3]	▬		**SmC$_A$***	87.7 [-0.04]	**SmC***	124.5 [-1.3]	**SmA***	125.9 [-3.6]	**Iso**	[56, 57, 87]
6.HF(*RAC*)	56.6 [+37.3]	106.1 [+4.4]	**Cr**	19.7§ [-30.5]	▬		**SmC$_A$**	70.0 [$^{@}$]	**SmC**	104.0 [-0.8]	**SmA**	105.1 [-4.2]	**Iso**	-
6.HF(*R*)	44.6 [+32.5]	104.5 [+4.9]	**Cr**	20.5§ [-30.2]	▬		**SmC$_A$***	68.9 [-0.04]	**SmC***	102.1 [$^{@}$]	**SmA***	102.8 [-4.8]	**Iso**	[56, 57, 87]
6.HF(*S*)	43.6 [+30.9]	105.5 [+4.9]	**Cr**	18.5§ [-30.4]	▬		**SmC$_A$***	67.3 [-0.03]	**SmC***	104.0 [-0.07]	**SmA***	104.3 [-5.0]	**Iso**	[56, 57, 87]
6.FH(*RAC*)	29.9 [+15.2]	115.3 [+4.5]	**Cr**	-5.0 [-8.7]	▬		**SmC$_A$**	72.0 [$^{@}$]	**SmC**	108.9 [-0.9]	**SmA**	114.1 [-4.4]	**Iso**	-
6.FH(*R*)	58.6 [+23.1]	113.9 [+4.0]	**Cr2**	-7.1 [-2.5]	**Cr1**	9.7 [-11.8]	**SmC$_A$***	73.6 [-0.01]	**SmC***	108.5 [-1.2]	**SmA***	112.4 [-3.9]	**Iso**	[56, 57, 87]
6.FH(*S*)	58.6 [+22.5]	113.8 [+3.8]	**Cr2**	-6.9 [-3.7]	**Cr1**	33.6 [6.5]	**SmC$_A$***	64.7 [-0.01]	**SmC***	108.6 [-0.9]	**SmA***	112.6 [-3.7]	**Iso**	[56, 57, 87]
6.FF(*RAC*)	70.8 [+23.6]	115.0 [+4.3]	**Cr**	39.7 [-20.4]	▬		**SmC$_A$**	100.4 [-0.02]	**SmC**	110.3 [-0.9]	**SmA**	113.7 [-4.2]	**Iso**	-
6.FF(*R*)	63.0 [+21.9]	113.8 [+3.9]	**Cr2**	33.4 [-16.5]	**Cr1**	42.6 [-0.4]	**SmC$_A$***	80.1 [-0.03]	**SmC***	110.4 [-1.0]	**SmA***	112.5 [-3.8]	**Iso**	[56, 57, 87]
6.FF(*S*)	64.3 [+22.5]	113.9 [+3.8]	**Cr**	34.1 [-17.7]	▬		**SmC$_A$***	77.8 [-0.04]	**SmC***	110.8 [-1.0]	**SmA***	112.8 [-3.7]	**Iso**	[56, 57, 87]

Notes and abbreviations: "–" - the phase does not exist; "§"– indicates that the peak corresponding to crystallization appeared in a further heating cycle; "@" – indicates that the phase transition possessed an enthalpy value under the resolution of the DSC apparatus and was detected by POM only; "Cr/Cr1/Cr2" – are the rigid crystal/liquid crystal modifications.

Figures

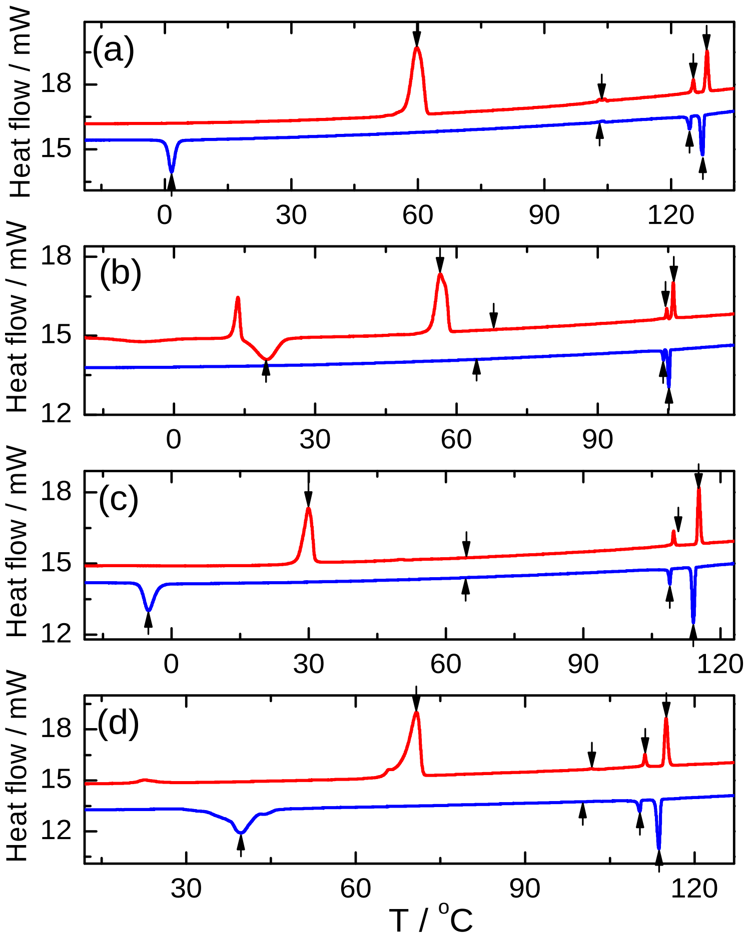

Figure 1.

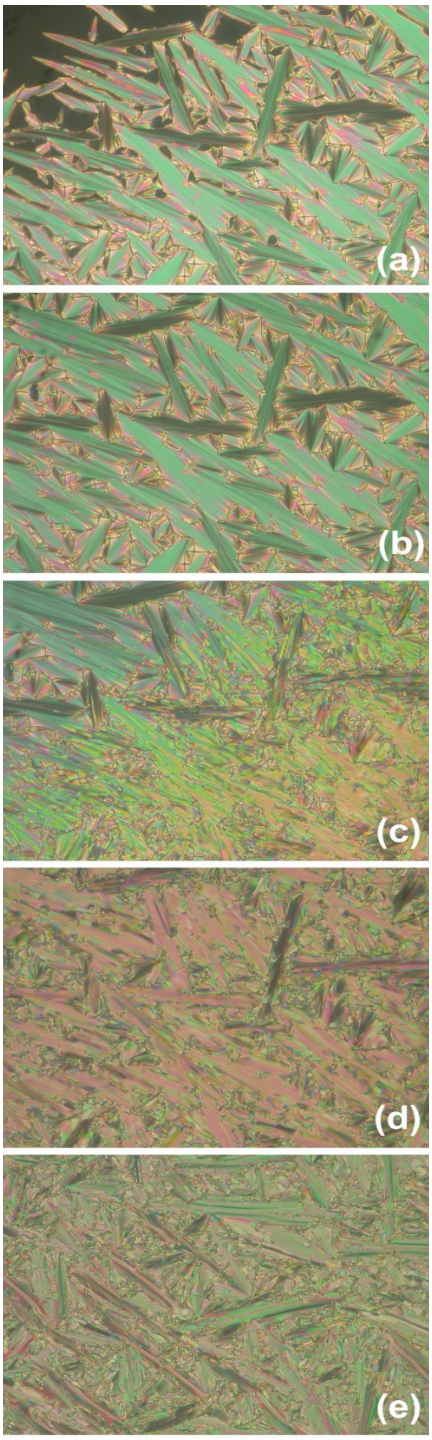

Figure 2.

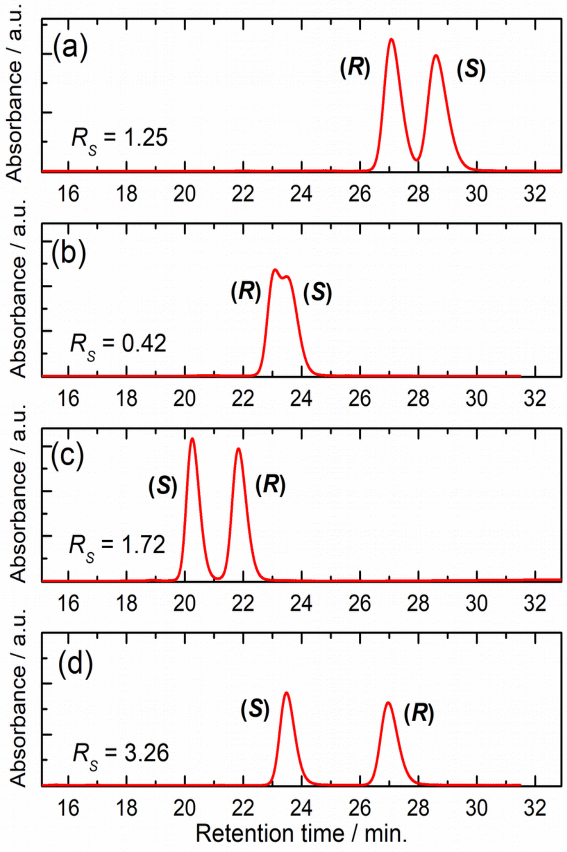
(a)
(R)
(S)
R_S = 1.25
(b)
(R)
(S)
R_S = 0.42
(c)
(S)
(R)
R_S = 1.72
(d)
(S)
(R)
R_S = 3.26
Absorbance / a.u.
16
18
20
22
24
26
28
30
32
Retention time / min.

Figure 3.

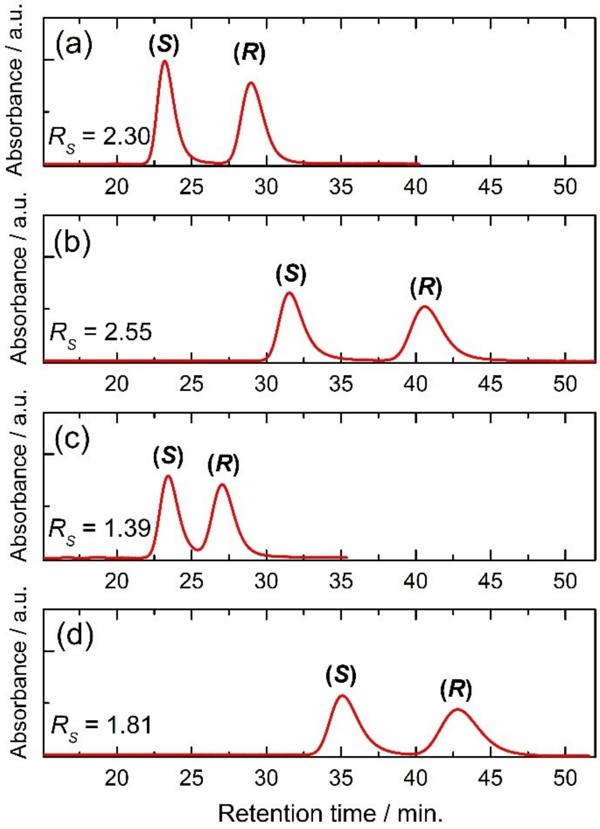
(a)
(S)
(R)
R_S = 2.30
(b)
(S)
(R)
R_S = 2.55
(c)
(S)
(R)
R_S = 1.39
(d)
(S)
(R)
R_S = 1.81
Absorbance / a.u.
20
25
30
35
40
45
50
Retention time / min.

Figure 4.

Figure captions

Figure 1. DSC plots of the heating/cooling runs (red/blue curves, respectively) for: 6.HH(RAC) (a), 6.HF(*RAC*) (b), 6.FH(*RAC*) (c) and 6.FF(*RAC*) (d) ester-based racemic materials. Vertical arrows indicate the peaks corresponding to phase transitions.

Figure 2. Microphotographs of the characteristic textures obtained from the cooling cycle for the 6.HH(*RAC*) ester material: (a) the Iso-SmA phase transition at approximately 127.5 °C; (b) the fan-shaped texture of the SmA phase at approximately 125.0 °C; (c) the SmA-SmC phase transition at approximately 124.5 °C; (d) the broken fan texture of the SmC phase at approximately 110.0 °C; and (e) the anticlinic $\mathrm{SmC_A}$ phase at approximately 50.0 °C. The width of all microphotographs is approximately 250 μm.

Figure 3. Chiral separations of 6.HH(*RAC*) (a), 6.HF(*RAC*) (b), 6.FH(*RAC*) (c) and 6.FF(RAC) (d) ester-based racemic materials on a CP column under the following separation conditions: mobile phase, hexane:IPA (98/2, v/v); flow rate, 1.0 $\mathrm{mL \cdot min^{-1}}$; and temperature, 20 °C.

Figure 4. Chiral separations of 6.HH(*RAC*) (a), 6.HF(*RAC*) (b), 6.FH(*RAC*) (c) and 6.FF(*RAC*) (d) ester-based racemic materials on an OJ column under the following separation conditions: mobile phase, hexane:IPA (98/2, v/v); flow rate, 1.0 $\mathrm{mL \cdot min^{-1}}$; and temperature, 40 °C.